Electronic Supplementary Material (ESI) for Dalton Transactions.
This journal is © The Royal Society of Chemistry 2021

Supporting Information

The construction of novel titanium oxide aerogel with highly enhanced removal of uranium and evaluated adsorption mechanism

Jun Liao[a,b], Yong Zhang[b *], Xiaoshan He[a], Lin Zhang[a], Zhibing He[a *]

[a] Division of Target Science and Fabrication, Research Center of Laser Fusion, China Academy of Engineering Physics, P. O. Box 919-987, Mianyang 621900, P. R. China.

[b] State Key Laboratory of Environmental-friendly Energy Materials & School of National Defence Science and Technology, Southwest University of Science and Technology, Mianyang 621010, P. R. China.

[*]Corresponding author. E-mail: hezhibing802@163.com (Z. He), pandmzy@foxmail.com (Y. Zhang).

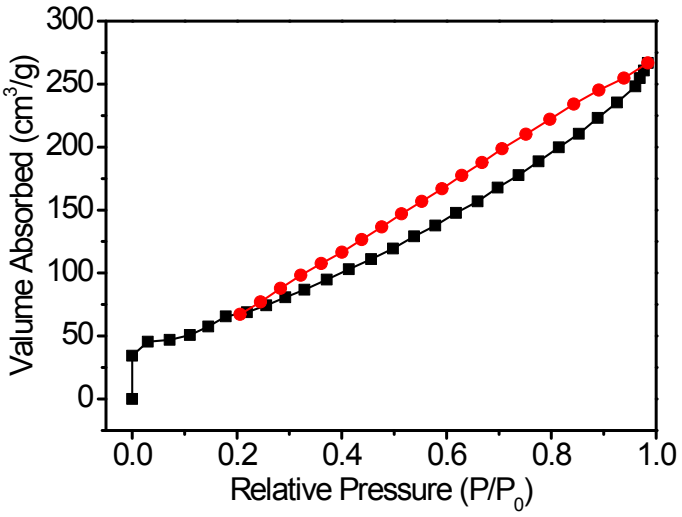

Figure S1. Nitrogen adsorption-desorption isotherms.

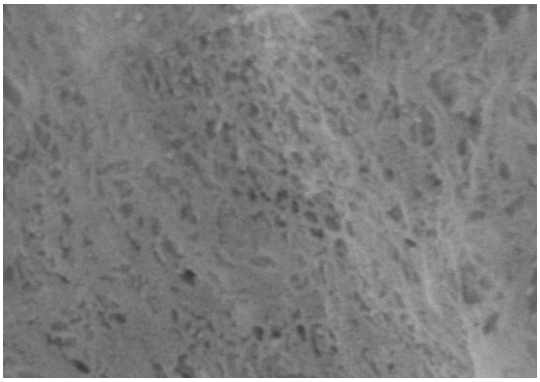

Figure S2. SEM images of TiO_2 aerogel.

The average crystallite sizes of TiO_2 aerogel were calculated from the main peaks of the X-ray line broadening of (101), (111) and (211) planes using the Scherrer equation.

$$D = \frac{0.89\lambda}{\beta \cos\theta}$$

where D is the average crystallite size (nm), θ is the diffraction angle (°), λ is the wavelength of X-ray (λ = 0.154 nm) and β is the full-width at half-maximum [S1, S2]. The parameter values for calculating crystal size were summarized in Table S1. According to the above data, the average diameter of TiO_2 particles was 24.0 nm.

Table S3. The parameter values for calculating crystal size.

Crystal plane	β	2θ (°)	D (nm)
(101)	0.40	36.1	24.3
(111)	0.41	41.2	25.5
(211)	0.61	54.3	22.1

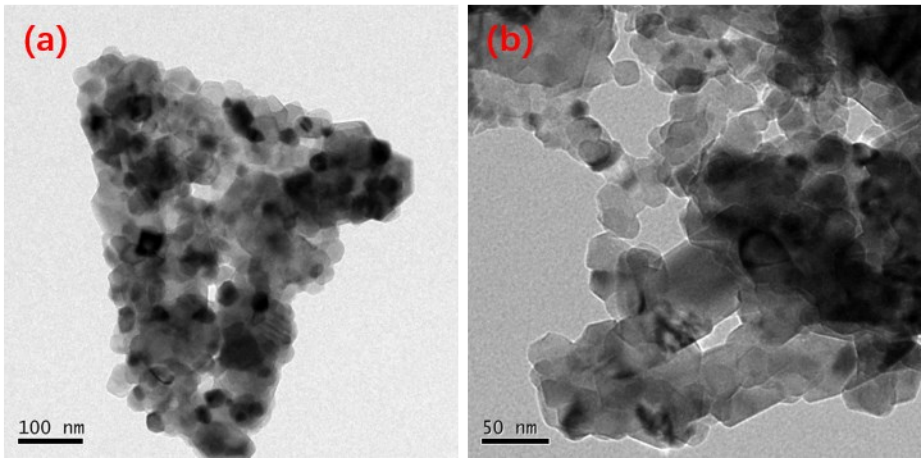

Figure S3. TEM images of TiO_2 aerogel.

Determination of the pH at zero charge point

In order to determine the pH of the adsorbent at the zero charge point, TiO_2 aerogel (10 mg) was stirred for 24 h in a KCl solution with a concentration of 0.1 M (10 mL). The initial pH of solution (pH 3-10) was adjusted with 0.1 M NaOH and 0.1 M HCl solution. After stirring, the final pH of the solution was measured by a pH meter. Subtracting initial pH values from equilibrium pH values, the ΔpH values were calculated. ΔpH values were placed on the y-axis and the initial pH values were placed on x-axis and a graph was drawn. The intersection of the graph and the x-axis is defined as pH_{zcp}.

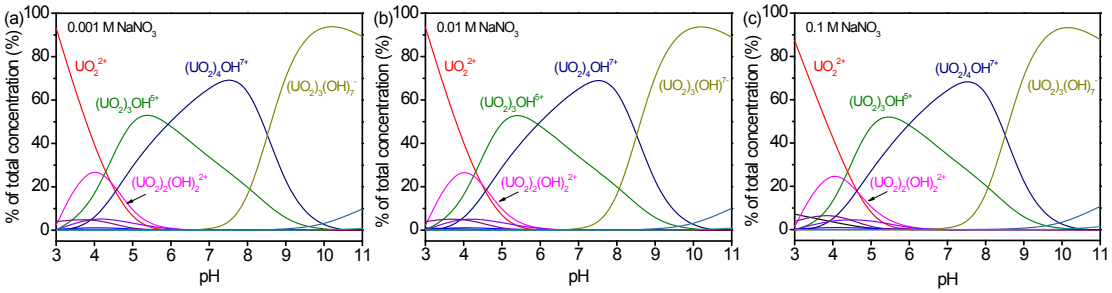

Figure S4. The influence of ion strength of NO_3^- on the existence of U(VI) species at different pH. (a) 0.001 M, (b) 0.01 M and (c) 0.1M.

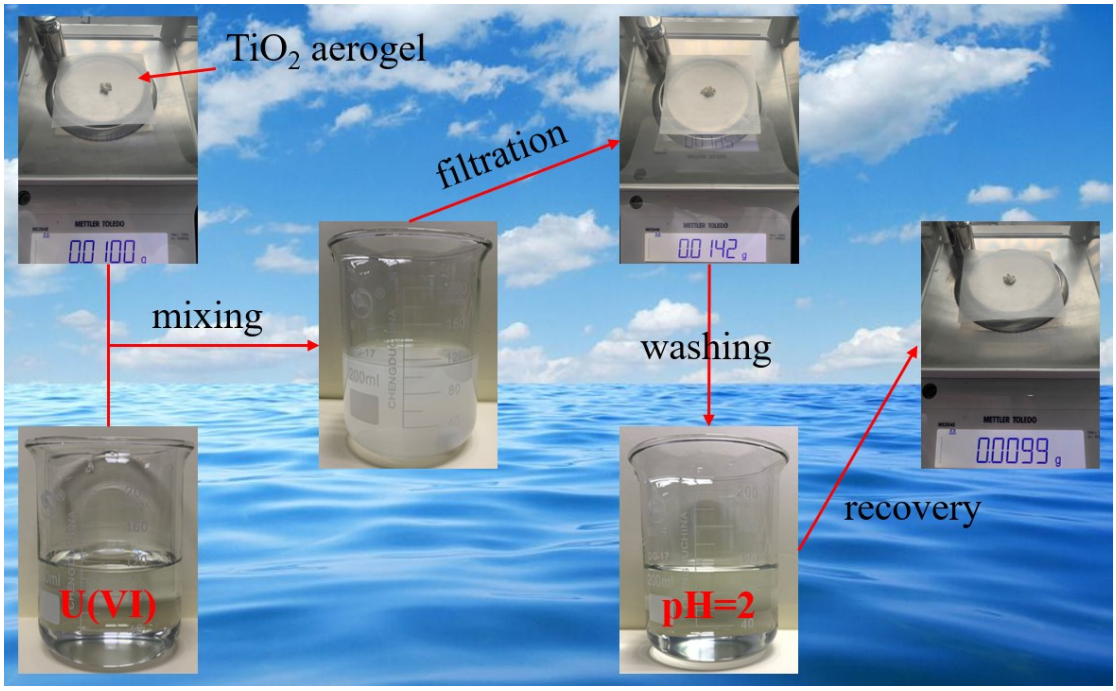

Figure S5. Recovery of TiO_2 aerogel.

Table S2. The recovery efficiencies of TiO_2 aerogel and desorption efficiencies of U(VI).

	Recovery efficiency (%)	Desorption efficiency (%)
1	98.3	99.8
2	98.0	99.8
3	97.6	99.1
4	97.1	99.3
5	97.1	99.0

Adsorption kinetics

Pseudo-first-order kinetic model

The adsorption kinetics of U(VI) on TiO_2 aerogel adsorbents was simulated by pseudo-first-order which were used to describe the physisorption behavior and it can be described by equations S1 and S2.

$$\text{linear: } \ln(q_e - q_t) = \ln q_e - k_1 t \tag{S1}$$

$$\text{non-linear: } q_t = q_e(1 - e^{-k_1 t}) \tag{S2}$$

Pseudo-second-order kinetic model

The pseudo-second-order presumed that the rate limiting step was essentially chemisorption and the mechanism might involve valence forces by sharing or through the exchange of electrons between adsorbate and adsorbent. It can be described by equations S3 and S4.

$$\text{linear: } \frac{t}{q_t} = \frac{1}{k_2 q_e^2} + \frac{t}{q_e} \tag{S3}$$

$$\text{non-linear: } q_t = \left(\frac{k_2 q_e^2 t}{1 + k_2 q_e t}\right) \tag{S4}$$

Elovich kinetic model

The Elovich kinetic model considered that the rate-controlling step is the diffusion of the target ions and it revealed the behaviors of chemisorption. The equation was given in the following:

$$q_t = \frac{1}{\beta}\ln(1 + \alpha\beta t) \tag{S5}$$

Intraparticle diffusion kinetic model

The intraparticle diffusion kinetic model assumed that the internal diffusion was a velocity-controlled step and the direction of diffusion is random. The equation was given in the following:

$$q_t = k_{ip} t^{0.5} + C_i \tag{S6}$$

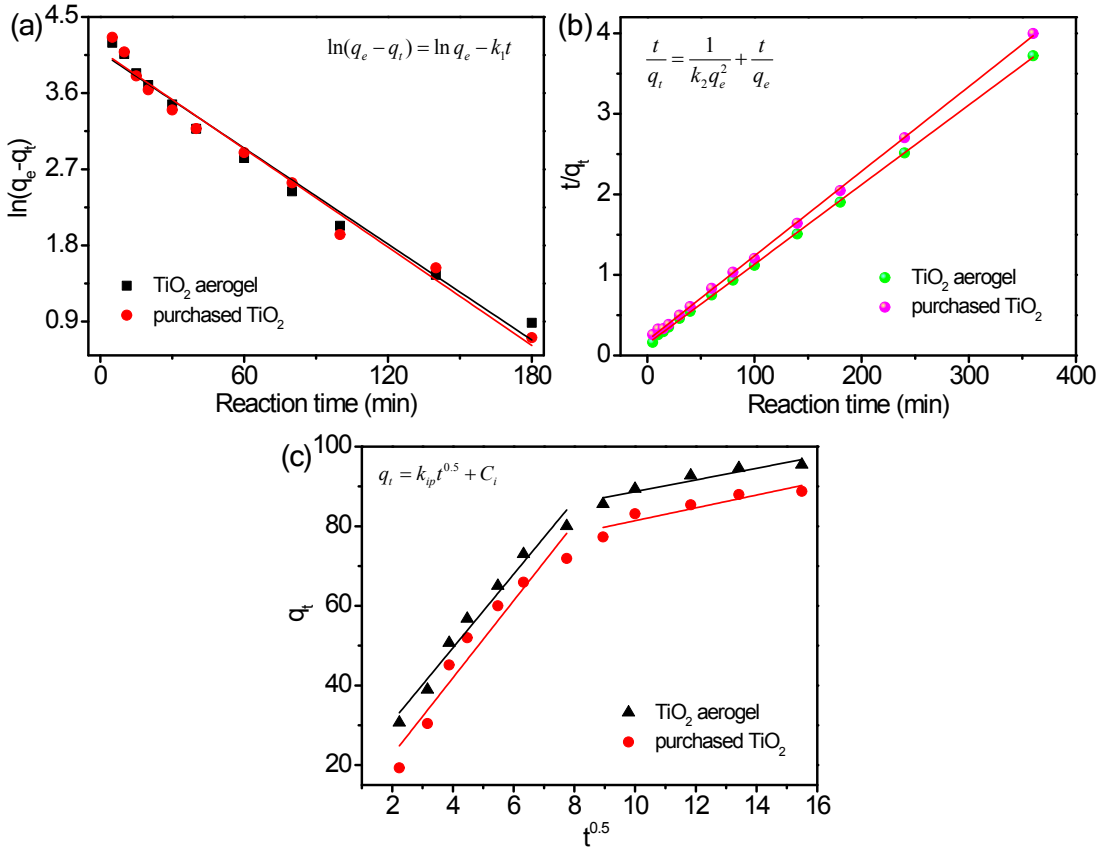

Figure S6. (a) linear pseudo-first-order kinetic model, (c) linear pseudo-second-order kinetic model and (c) intraparticle diffusion kinetic model (C_0 = 10 mg/L, m/V = 0.1 g/L, pH = 5).

Isotherm model

Langmuir isotherm model

The Langmuir model assumes that monolayer adsorption takes place on the homogenous surfaces. It is one of the most widely used isotherm in adsorption. The linear and nonlinear forms of the Langmuir model is given by the following equations.

$$\text{linear: } \frac{C_e}{q_e} = \frac{1}{K_L q_m} + \frac{C_e}{q_m} \tag{S7}$$

$$\text{non-linear: } q_e = \frac{q_m K_L C_e}{1 + K_L C_e} \tag{S8}$$

Freundlich isotherm model

The Freundlich model has been regarded as an empirical equation without physical meaning. In many published papers, the Freundlich isotherm was applied to represent the multilayer adsorption on heterogamous surfaces. The Freundlich isotherm model can be described by equations S9 and S10.

$$\text{linear: } \ln q_e = \ln K_F + \frac{1}{n} \ln C_e \tag{S9}$$

$$\text{non-linear: } q_e = K_F C_e^{\frac{1}{n}} \tag{S10}$$

Sips isotherm model

The Sips model is hybrid model combining the Langmuir and Freundlich models and it is the most applicable 3-parameter isotherm model for monolayer adsorption. Besides, the Sips model can describe the homogeneous or heterogeneous systems. It is presented by equation S11.

$$q_e = \frac{q_m K_S C_e^{n_S}}{1 + K_S C_e^{n_S}} \tag{S11}$$

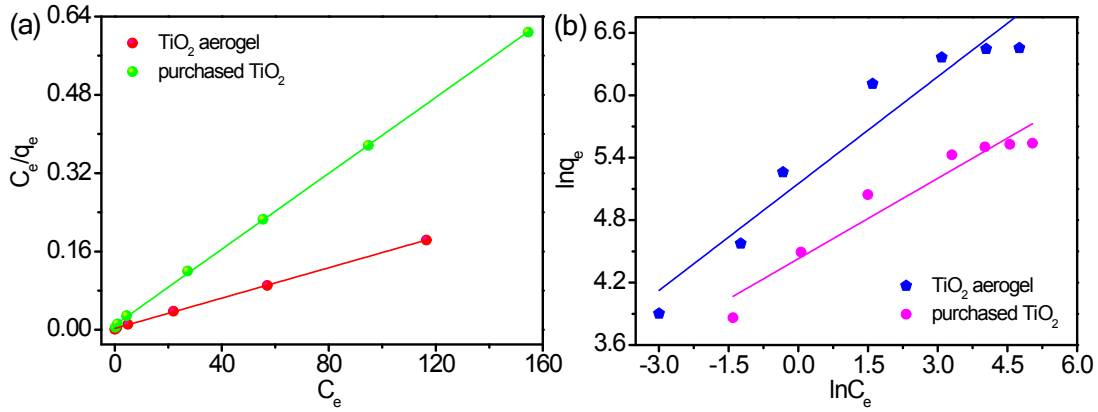

Figure S7. (a) linear Langmuir model and (b) linear Freundlich model (m/V = 0.1 g/L, pH = 5).

Table S3. Comparison of the maximum adsorption capacity of U(VI) on various adsorbents.

Adsorbents	T (K)	pH	Capacity (mg/g)	References
$CaTiO_x$	298	4	241.71	[6]
MnO_2@TiO_2	298	5	105.3	[28]
3D GA/TiO_2	298	5	441.3	[29]
PVA/TiO_2 nanofiber	318	4.5	196.1	[30]
defective TiO_{2-x}	298	5.0	65	[31]
PA/TNTs	293	5	276.1	[35]
TiO_2 aerogel	298	5	638.0	This work

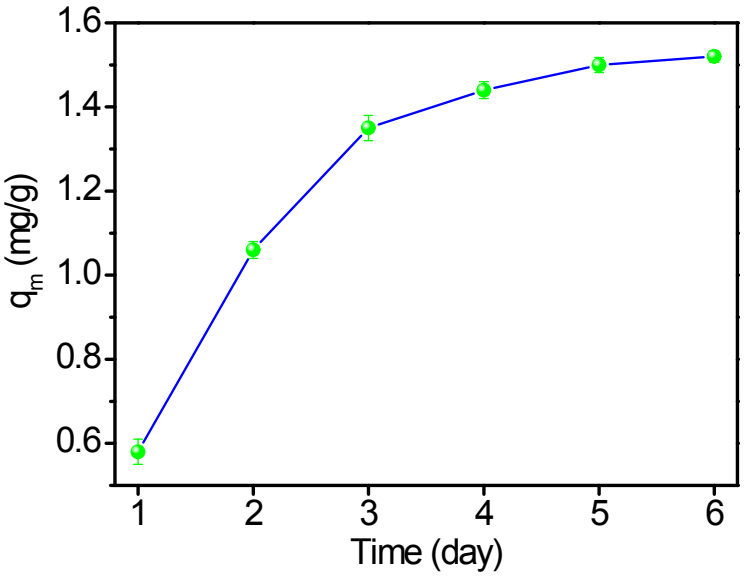

Figure S8. Adsorption kinetics of TiO_2 aerogel in 30 L of natural seawater.

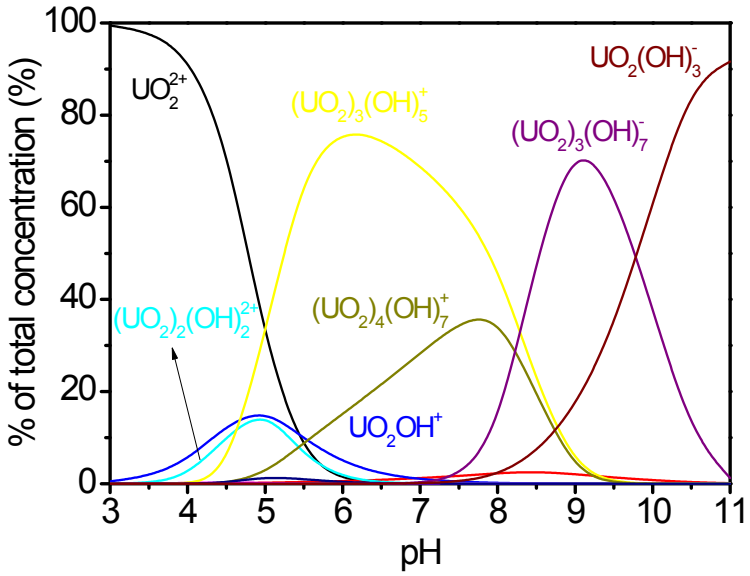

Figure S9. The existence of U(VI) species in the pH range of 3~11.

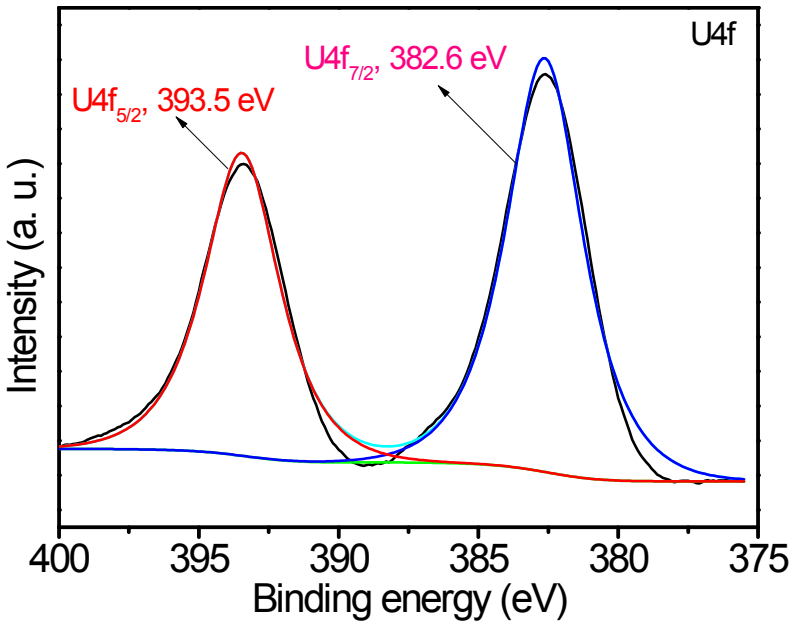

Figure S10. High-resolution XPS spectra of U4f.

References

[S1]Duangchuen, T., Karaphun, A., Wannasen, L., Kotutha, I., Swatsitang, E., 2019. Effect of SnS_2 concentrations on electrochemical properties of SnS_2/RGO nanocomposites synthesized by a one-pot hydrothermal method. Applied Surface Science, 487, 634-646.

[S2]Li, D., Wang, H., Wang, X., 2007. Effect of microstructure on the modulus of PAN-based carbon fibers during high temperature treatment and hot stretching graphitization. Journal of Materials Science, 42, 4642-4649.